Thermal processes in metal-coated fiber probes for near-field experiments

A. Ambrosio[a] and M. Allegrini
Dipartimento di Fisica "E. Fermi", Universitá di Pisa, Largo Pontecorvo 3, I-56127 Pisa, Italy

G. Latini[b] and F. Cacialli
Department of Physics and Astronomy, University College London, and London Centre for Nanotechnology, Gower Street, WC1E 6BT, London, United Kingdom

(Received 15 February 2005; accepted 7 June 2005; published online 13 July 2005)

We have used a ray optics model to calculate the optical power absorbed in the metal coating of apertured probes for scanning near-field optical microscopy. We have then introduced the absorbed power profile into the heat balance equation to calculate the temperature of the probe as a function of the distance from the apex. By comparing our results with available experimental data, we demonstrate accurate prediction of both the temperature profile along the probe, and the temperature increase per mW of power launched into the fiber (60.7 versus 60 K/mW at 25 μm from the apex). © *2005 American Institute of Physics*. [DOI: 10.1063/1.1999019]

The thermal regime of apertured probes[1] for scanning near-field optical microscopes (SNOM) (Refs. 2 and 3) can significantly affect the results of both imaging or spectroscopic observations,[4] and of near-field lithography experiments.[5]

Scanning near-field optical lithography[6–11] is gaining increasing momentum as an affordable technique suitable for the direct writing of a variety of nano- and mesostructures, especially of photosensitive organic functional materials. For such applications, it is crucial to achieve a detailed understanding of potential thermolithographic effects, which should not degrade the resolution of patterning by interfering with the materials' photochemistry.

Several groups[12,13] have reported substantial heating of apertured probes, up to several hundred degrees, owing to light absorption by the probe metal coating. This may affect the fiber throughput[14] and determine a relatively fast elongation of the fiber end.[4,15–18] In the last ten years, significant efforts have also been devoted to understanding the heating mechanisms of SNOM probes, with a view to finding ways to prevent the concomitant effects. A repeated-zone model[19,20] has provided a first description of the relevant heating phenomena and has allowed calculation of the power absorbed along the axis of the SNOM fiber. In other cases,[21] a more general ray-tracing model has been used to take into account different probe geometries.

In this letter, we calculate the power absorbed along a SNOM probe with a conical shape and then use such an absorption profile in combination with the heat balance equation to estimate the temperature of the probe along the fiber length.

For our calculation, we model the probe as a collection of slices of thickness dz. For each slice, we can write the following heat balance equation:

$$\frac{\partial}{\partial t}\frac{\partial Q(z)}{\partial z} = \frac{\partial P(z)}{\partial z} - \frac{\partial J_{\mathrm{conv}}(z)}{\partial z} - \frac{\partial J_{\mathrm{diff}}(z)}{\partial z}, \tag{1}$$

where we adopt the same symbol convention as Gucciardi *et al.*,[18] namely: $[\partial Q(z)/\partial z]dz$ is the heat in the slice centered at position z along the fiber axis; $[\partial P(z)/\partial z]dz$ is the optical power absorbed by the slice walls; $[\partial J_{\mathrm{conv}}(z)/\partial z]dz$ is the heat transfer from the slice to the environment by thermal convection (in the unit time); and $[\partial J_{\mathrm{diff}}(z)/\partial z]dz$ is the heat exiting the slice via conduction through the metallic coating, in the unit time.

We consider a bundle of optical rays with a circular section (with radius R), entering the base of the conical taper and suffering several consecutive reflections by the metal film on the cone walls. In our analysis, we have started to calculate the z coordinates (z_n) of the points where the more external rays of the bundle impinge on the metal coating after n previous reflections, as schematically shown in Fig. 1. With the help of Fig. 1, we find that

$$z_n = \frac{R\cos\alpha}{\sin(\beta + 2n\alpha)} \tag{2}$$

where α is the half angle of the cone, β is the initial inclination of the rays with respect to the fiber walls, and R is the

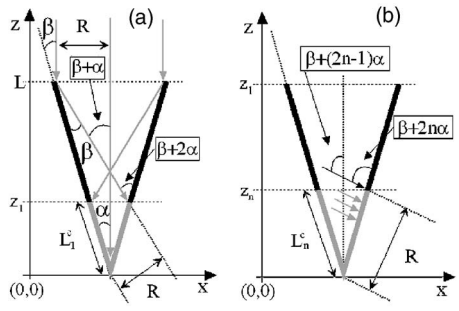

FIG. 1. (a) Schematic representation of the multiple reflections of the light rays in the SNOM fiber-end hot region of length L. The radius of the ray bundle (with circular section) is R. Note that the metalized cone walls reflect light rays as mirrors and keep R constant. (b) The reflections of the more external rays define the quotes z_n and the cone lateral area illuminated by the nth reflected bundle of rays (gray section in the picture). After n reflections, the angle of the bundle with the cone axis is $\beta+(2n-1)\alpha$. The quotes z_n are then found through the relations: $L_n^c=[R/\sin(\beta+2n\alpha)]$;$L_n^c\cos(\alpha)=z_n$.

[a]Electronic mail: ambrosio@df.unipi.it
[b]Current address: Istituto dei Sistemi Complessi-Consiglio Nazionale delle Ricerche, Via Fosso del Cavaliere, 100-00133 Rome, Italy.

radius of the circular bundle entering the cone (R is equal to the cone base radius only if $\beta=\alpha$). In general, for nonconical probes, the coordinates z_n may be calculated as the intersection of the straight lines describing the optical rays and a polynomial describing the metal coating.[21] After n reflections, the ray bundle transports a partial power of $(1-\gamma)^n P_0$, where γ is the absorption coefficient of the metal coating ($\gamma=8\%$ for aluminum in the visible wavelengths region), and P_0 is the total power entering the conical fiber end. The rays reflected n times illuminate a conical area of the coating equal to $A_n^{\text{impact}}=\pi z_n \tan\alpha(z_n/\cos\alpha)$, shown in gray in Fig. 1. Because of the probe conical shape, the optical power is not uniformly distributed on such areas, but decreases as $W_n(z)=(z^2/z_n^2)$. Thus, the intensity along z of the bundle reflected n times is

$$I_n(z)=\begin{cases} P_0(1-\gamma)^n \sin(\beta+2n\alpha)(1/A_n^{\text{impact}})W_n(z) & \text{if } 0\leqslant z\leqslant z_n \\ 0 & \text{if } z_n<z\leqslant L \end{cases} \tag{3}$$

where L is the length of the conical taper (Fig. 1) and the factor $\sin(\beta+2n\alpha)$ is introduced to consider only the flux perpendicular to the cone walls.

The lateral area of each cone slice of thickness dz is $A^{\text{lat}}=2\pi z \tan\alpha(dz/\cos\alpha)$. The power of the nth reflected rays that is absorbed by the slice at quote z is, therefore,

$$p_n(z)=\gamma I_n(z)A^{\text{lat}}. \tag{4}$$

Combining the previous expressions we are now able to write the absorbed power profile function $\partial P(z)/\partial z$ as

$$\frac{\partial P(z)}{\partial z}=\sum_{n=0}^{N} p_n(z)=\sum_{n=0}^{N} 2\gamma(1-\gamma)^n P_0 \frac{z}{z_n^2}\frac{z^2}{z_n^2}\sin(\beta+2n\alpha), \tag{5}$$

where the sum must be extended over the total number N of forward and backward reflections. In Fig. 2(a), we report the behavior of $\partial P(z)/\partial z$ versus z for different probe shapes (different values of α) and for a fixed laser power $P_0=1$ mW entering the conical tip. As the tip gets sharper (decreasing α), the maximum increases and gets closer to the apex, in agreement with previous work.[20] This phenomenon may appear counterintuitive, but can in fact be explained easily within our model by considering the crucial role of the backreflections. For sharper tips, the total number of reflections N increases, and the position where the backreflections start from gets closer to the apex. Therefore, the point at which the sum of the optical power losses reaches a maximum also moves closer to the tip apex.

The results here reported are encouraging, although the model is not yet complete, because so far we have only considered a single bundle, characterized by a single propagation direction. In fact, rays can propagate in a fiber with a distribution of angles (measured with respect to the fiber axis) up to the critical angle. To account for the possible propagation directions, we have considered ten bundles characterized by different propagation angles (β) in the range 0°–10°, and then substituted $\partial P(z)/\partial z$ in Eq. (1) with a weighted sum of $\partial P(z)/\partial z$ calculated for such ten angles. The weights were selected according to a Gaussian distribution, and account for the fact that the surface density of rays (optical flux) decreases with increasing inclination with respect to the optical axis. The plot of the function substituted to $\partial P(z)/\partial z$ in Eq. (1), is reported in Fig. 2(b).

To check the validity of our model, we have applied it to the case of an aluminum-coated probe with $\alpha=3°34'48''$, $L=1$ mm, and $P_0=3.3$ mW, whose temperature profile has been reported by Stähelin and co-workers.[12] In this case, we have considered Eq. (1) at steady state $[\partial/\partial t(\partial Q(z)/\partial z)=0]$ and turned the heat balance equation into a second-order differential equation for the temperature profile function by expressing each term in Eq. (1) as function of $T(z)$.[18] As boundary conditions, of the heat balance equation, we have then taken $\partial T/\partial z=0$ at the tip apex (i.e., $z=0$), as in Ref. 22, whereas for the fiber shaft (from L on), we have considered a fix temperature of 34 °C, as measured in Ref. 12. The calculated temperature profile is shown in Fig. 3 (solid line) and is in excellent agreement with the experimental data[12] (dots). The agreement could perhaps be even better if all the experimental parameters were known, such as the fiber numerical aperture, here assumed to be 0.17 and corresponding to a maximum $\beta\sim 10°$. Note that the temperature is maximum in the region of the tip apex even though the point of maximum

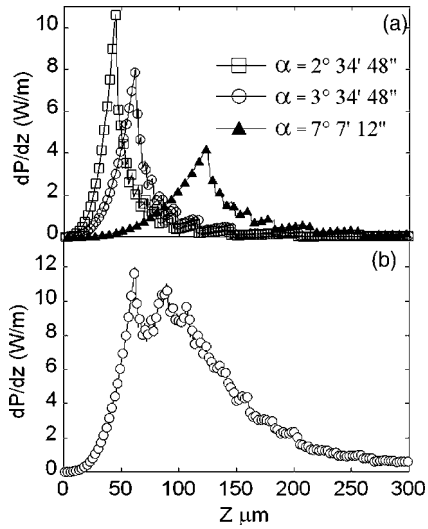

FIG. 2. (a) Power absorbed by a fiber slice of thickness dz as a function of the quote z. Note that the maximum is greater for smaller angles ($\alpha=2°34'48''$, $L=1$ mm), i.e., is for sharper conical profiles. Due to multiple reflections by the cone walls, light is focused close to the tip apex. Note that the focusing effect is greater for sharper tips (smaller angles). (b) Graphical representation of the power absorbed by a fiber slice of thickness dz as a function of the quote z in the case of a weighted distribution of ten angles in the range 0–10°.

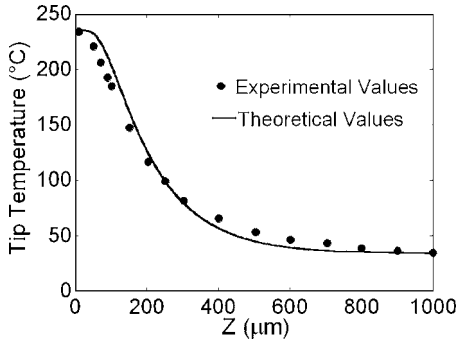

FIG. 3. Calculated (solid line) and measured (dots) probe temperature profile for an aluminum coated probe with $\alpha=3°34'48''$, $L=1$ mm, and $P_0=3.3$ mW. The experimental temperature profile is taken from previously reported data (Ref. 12).

absorbance is slightly displaced from the apex. This may appear counterintuitive, but is in fact consistent with the expected loss of efficiency of the dissipative mechanisms J_{conv} and J_{diff} due to the small dimensions of the apical region.

As an additional check of the validity of our model, we have also calculated the coefficient describing the probe temperature increase per unit power of optical radiation (K/mW). We found that the coefficient is 60.7 K/mW at 25 μm from the tip apex, in excellent agreement with that measured by Stähelin and collaborators[12] of 60 K/mW in the same conditions. Using the function $\partial P(z)/\partial z$, we have evaluated that most of the power (about 99.9%) is absorbed in the region where the fiber diameter is greater than one-half of a wavelength of injected light. This is why our simple model leads to surprising agreement with experimental data despite neglecting the evanescent nature of the electromagnetic field at the tip apex.

Our description provides important information for the understanding of the potential influence of thermal effects in apertured near-field lithography processes.[5] More generally, a simple evaluation of the tip temperature, as that reported here, is of general interest for apertured near-field microscopy, although additional effects, and in particular heat transfer from the surrounding medium or to the sample surface should be taken into account by considering other dissipative channels in Eq. (1).[23,24]

The authors would like to acknowledge financial support from MIUR-National FIRB project "Nanotechnologies and Nanodevices for the Information Society", from the Royal Society, EPSRC, and the Interdisciplinary Research Collaboration in Nanotechnology.

[1] J. A. Veerman, A. M. Otter, L. Kuipers, and N. F. van Hulst, Appl. Phys. Lett. **72**, 3115 (1998).
[2] D. W. Pohl, W. Denk, and M. Lanz, Appl. Phys. Lett. **44**, 651 (1984).
[3] A. Lewis, M. Isaacson, A. Harootunian, and A. Muray, Ultramicroscopy **13**, 227 (1984).
[4] C. Lienau, A. Richter, and T. Elsaesser, Appl. Phys. Lett. **69**, 325 (1996).
[5] G. Latini, A. Downes, O. Fenwick, A. Ambrosio, M. Allegrini, C. Daniel, C. Silva, P. G. Gucciardi, S. Patanè, R. Daik, W. J. Feast, and F. Cacialli, Appl. Phys. Lett. **86**, 011102 (2005).
[6] R. Riehn, A. Charas, J. Morgado, and F. Cacialli, Appl. Phys. Lett. **82**, 526 (2003).
[7] X. Yin, N. Fang, X. Zhang, I. B. Martini, and B. J. Schwartz, Appl. Phys. Lett. **81**, 3663 (2002).
[8] S. Q. Sun and G. J. Leggett, Nano Lett. **2**, 1223 (2002).
[9] D. Richards and F. Cacialli, Philos. Trans. R. Soc. London, Ser. A **362**, 771 (2004).
[10] F. Cacialli, R. Riehn, A. Downes, G. Latini, A. Charas, and J. Morgado, Ultramicroscopy **100**, 449 (2004).
[11] E. Betzig and J. K. Trautman, Science **257**, 189 (1992).
[12] M. Stähelin, M. A. Bopp, G. Tarrach, A. J. Meixner, and I. Zschokke-Gränacher, Appl. Phys. Lett. **68**, 2603 (1996).
[13] L. Thiery, N. Marini, J. P. Prenel, M. Spajer, C. Bainier, and D. Courjon, Int. J. Therm. Sci. **39**, 519 (2000).
[14] B. I. Yakobson, A. LaRosa, H. D. Hallen, and M. A. Paesler, Ultramicroscopy **61**, 179 (1995).
[15] D. I. Kavaldjiev, R. Toledo-Crow, and M. Vaez-Iravani, Appl. Phys. Lett. **67**, 2771 (1995).
[16] A. H. La Rosa, B. I. Yakobson, and H. D. Hallen, Appl. Phys. Lett. **67**, 2597 (1995).
[17] B. Biehler and A. H. La Rosa, Rev. Sci. Instrum. **73**, 3837 (2002).
[18] P. Gucciardi, M. Colocci, M. Labardi, and M. Allegrini, Appl. Phys. Lett. **75**, 3408 (1999).
[19] B. I. Yakobson and M. A. Paesler, Ultramicroscopy **57**, 204 (1995).
[20] L. Thiery and N. Marini, Ultramicroscopy **94**, 49 (2003).
[21] L. Thiery, N. Marini, C. Bainier, and D. Charraut, Opt. Eng. (Bellingham) **40**, 1010 (2001).
[22] S. Grafstrom, P. Schuller, J. Kowalski, and R. Neumann, J. Appl. Phys. **83**, 3453 (1998).
[23] P. I. Geshev, F. Demming, J. Jersch, and J. Dickmann, Appl. Phys. B: Lasers Opt. **70**, 91 (2000).
[24] J. L. Kann, T. D. Milster, F. F. Froehlich, R. W. Ziolkowski, and J. B. Judkins, Appl. Opt. **36**, 5951 (1997).